https://doi.org/10.3311/PPme.19424

Periodica Polytechnica Mechanical Engineering, 66(3), pp. 219–230, 2022

Establishment of Impulsive and Accelerated Motions of Casson Fluid in an Inclined Plate in the Proximity of MHD and Heat Generation

Malapati Venkateswarlu[1*], Meduri Phani Kumar[2], Oluwole Daniel Makinde[3]

[1] Department of Mathematics, Velagapudi Ramakrishna Siddhartha Engineering College, 520 007 Vijayawada, Andhra Pradesh, India
[2] Department of Mathematics, VIT-AP University, 522 237 Amaravathi, Andhra Pradesh, India
[3] Faculty of Military Science, Stellenbosch University, Private Bag X2, 7395 Saldanha, South Africa
[*] Corresponding author, e-mail: mvsr2010@gmail.com

Received: 20 October 2021, Accepted: 20 June 2022, Published online: 30 June 2022

Abstract

This article is committed to examine the unsteady MHD Casson liquid flow in an inclined infinite vertical plate in the proximity of heat generation and thermal radiation. The governing energy and momentum partial differential equations are ascertained. The momentum equation is established for two distinct types of conditions when the magnetic domain is relevant to the liquid and the magnetic domain is relevant to the moving plate. Analytical expressions for liquid temperature and motion are acquired by applying Laplace transform technique. The effects of physical parameters are accounted for two distinct types of motions namely impulsive motion and accelerated motion. The numerical values of liquid motion and temperature are displayed graphically for various values of pertinent flow parameters. A particular case of our development shows an excellent compromise with the previous consequences in the literature.

Keywords

hydromagnetic, impulsive motion, accelerated motion, heat generation, radiation, inclined plate

1 Introduction

In real-life operations several products such as paints, shampoos, compressed milk, publish ink, and tomato cream, etc., exhibit disparate properties that cannot be instinctively accepted by the Newtonian concept. So, to characterize such kind of liquids it is required to present the concept of non-Newtonian liquid. In 1995, Casson fluid pattern was developed by Casson [1]. Poornima et al. [2] reported the radiation and chemical reaction contributes on Casson non-Newtonian liquid in the proximity of thermal and Navier slip constraints towards a stretching facade. Aboalbashari et al. [3] obtained the entropy formation equation in terms of velocity, temperature, and concentration gradients. Makinde and Eegunjobi [4] observed that the influence of magnetic domain and Casson liquid parameter have significant reaction on the entropy generation rate. Reddy et al. [5] performed the hydromagnetic stream of Casson nanoliquid towards a cylinder in the proximity of first order velocity, thermal, and concentration Biot conditions. Shashikumar et al. [6] informed that the entropy production rate escalates with an enhancement in radiation parameter and Biot number. Gireesha et al. [7] presented the entropy production and heat transmit inspection of Casson liquid stream in the proximity of viscous and Joule warming in an inclined micro-porous-channel. Kalyan Kumar and Srinivas [8] presented the consequence of joule warming and radiation on unsteady MHD stream of chemically responding Casson liquid through a slantwise stretching plate. Venkateswarlu and Bhaskar [9] reported the entropy generation and Bejan number analysis of MHD Casson fluid flow in a micro-channel with Navier slip and convective boundary conditions. Goud et al. [10] presented the thermal radiation and Joule heating effects on a MHD Casson nanofluid flow in the presence of chemical reaction through a non-linear inclined porous stretching sheet.

Hydromagnetic is an exploration of the microscopic interaction of electrically administrating liquid and gas with the magnetic domain. It has several significant applications in science and engineering, for instance, wind energy, astrophysics, aerospace, solar energy collectors, nuclear reactors, electromagnetics, transformers, geomechanics,

Cite this article as: Venkateswarlu, M., Phani Kumar, M., Makinde, O. D. "Establishment of Impulsive and Accelerated Motions of Casson Fluid in an Inclined Plate in the Proximity of MHD and Heat Generation", Periodica Polytechnica Mechanical Engineering, 66(3), pp. 219–230, 2022.
https://doi.org/10.3311/PPme.19424

oceanography, electrical heaters, plasma confinement, magnetic drug targeting, geophysics, etc. Cramer and Pai [11] documented the magnetofluid dynamics for engineers and applied physicists. Malapati and Polarapu [12] presented the unsteady MHD free convective heat and mass transfer in a boundary layer flow past a vertical permeable plate with thermal radiation and chemical reaction. Yahiaoui et al. [13] reported the investigation of the mixed convection from a confined rotating circular cylinder. Mami and Bouaziz [14] considered the effect of MHD on nanofluid flow, heat and mass transfer over a stretching surface embedded in a porous medium. Venkateswarlu et al. [15] presented the thermodynamic analysis of Hall current and Soret number on hydromagnetic couette flow in a rotating system with a convective boundary condition.

Thermal radiation is a process by which energy is emitted directly from the radiated surface in the form of an electromagnetic wave in all directions. From the engineering and physical point of view, thermal radiation impact has a pivotal role in the flow of different liquid and heat transmit. Thermal radiation is found to be useful in engineering processes which require high operating temperature. These include; the design of the nuclear plant, gas turbine, aircraft, space vehicle, reliable equipment, satellite etc. Makinde and Ogulu [16] reported the significance of thermal radiation on the heat and mass transfer stream of an unstable viscosity liquid past a vertical porous wall suffuse by a transverse magnetic domain. Bagheri et al. [17] presented the viscous heating effects on heat transfer characteristics of an explosive fluid in a converging pipe. Cao and Baker [18] discussed the non continuum significance on natural convection radiation boundary layer stream from a warmed vertical wall. Das and Sarkar [19] analyzed the significance of melting on an MHD micropolar liquid stream toward a shrinking sheet with thermal radiation. Ymeli et al. [20] presented the analytical layered solution of radiation and non-Fourier conduction problems in optically complex media. Ferroudj et al. [21] discussed the Prandtl number effects on the entropy generation during the transient mixed convection in a square cavity heated from below. Venkateswarlu and Lakshmi [22] discussed the diffusion-thermo and heat source effects on the unsteady radiative MHD boundary layer slip flow past an infinite vertical porous plate.

Regarding the significance of an inclined channel several reports have been prepared by various researchers. Alam et al. [23] presented the effects of variable suction and thermophoresis on steady MHD combined free-forced convective heat and mass transfer flow over a semi infinite permeable inclined plate in the presence of thermal radiation. Makinde [24] reported the thermodynamic second law analysis for a gravity driven variable viscosity liquid film along an inclined heated plate with convective cooling. Venkateswarlu and Makinde [25] considered the unsteady MHD slip flow with radiative heat and mass transfer over an inclined plate embedded in a porous medium. Venkateswarlu et al. [26] presented the Soret and Dufour effects on radiative MHD flow of a chemically reacting fluid over an exponentially accelerated inclined porous plate in presence of heat absorption and viscous dissipation. Reddy et al. [27] presented the heat and mass transfer of a peristaltic electro-osmotic flow of a couple stress liquid through an inclined asymmetric channel with effects of thermal radiation and chemical reaction.

The objective of the present work is to record the effects of pertinent parameters governing the Casson liquid flow and to discuss the work of Chandran et al. [28] as a particular case. They are not considered the impact of angle of inclination, heat generation and thermal radiation. The following strategy is pursued in the rest of the paper. Section 2 presents the formation of the problem. The analytical solutions are presented in Section 3. Results are discussed in Section 4 and finally Section 5 provides a conclusion of the paper.

2 Formation of the problem

In this article, we consider an unsteady hydromagnetic flow of a viscous, incompressible, and radiating Casson fluid of Prandtl number equal to unity past an inclined infinite plate. The x-axis is taken along the plate in the upward direction and the y-axis is taken normal to it. The plate is inclined to vertical direction by an angle α. Magnetic domain of intensity B_0 is applied in the y-direction. At time $t = 0$, the plate and the liquid medium are at rest and at the constant temperature T_∞. At time $t > 0$, the plate is set into motion with a velocity $u_0 t^n$ and heat is also supplied to the plate at a constant rate. Two distinct flow cases will be taken here with regarding to the magnetic force. The first regarding to the case when the magnetic lines of force are fixed relative to the fluid, and the second to the case when the magnetic lines of force are fixed relative to the moving plate. The physical model is represented in Fig. 1.

The rheological equation of extra stress tensor for an isotropic and incompressible stream of a Casson liquid can be expressed in [10] as

$$\tau_{ij} = \begin{cases} 2\left(\mu_B + P_y \big/ \sqrt{2\pi}\right) e_{ij}, & \pi > \pi_c \\ 2\left(\mu_B + P_y \big/ \sqrt{2\pi_c}\right) e_{ij}, & \pi < \pi_c \end{cases}.$$

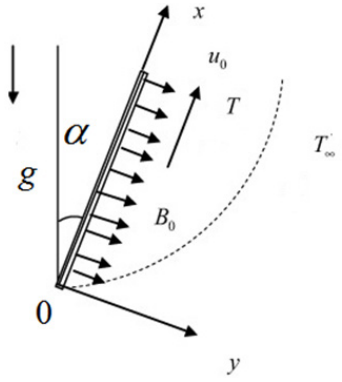

Fig. 1 Sketch of an inclined infinite vertical plate

Here μ_B is the plastic dynamic viscosity of non-Newtonian liquid, P_y is the yield stress of the liquid, π is the product of the component of the deformation rate with itself, namely, $\pi = e_{ij}e_{ij}$, e_{ij} is the $(i, j)^{\text{th}}$ component of the deformation rate, and π_c is the critical value of π based on non-Newtonian model.

Following Chandran et al. [28], the boundary layer equations of momentum and heat transfer past an inclined plate can be expressed in the pattern:

- Momentum equation:

$$\frac{\partial u}{\partial t} = \nu\left(1+\frac{1}{\beta}\right)\frac{\partial^2 u}{\partial y^2} + g\beta\left(T-T_\infty\right)\cos(\alpha) - \frac{\sigma B_0^2}{\rho}u\,, \quad (1)$$

- Energy equation:

$$\frac{\partial T}{\partial t} = \frac{k_T}{\rho c_p}\frac{\partial^2 T}{\partial y^2} - \frac{1}{\rho c_p}\frac{\partial q_r}{\partial y} + \frac{Q\left(T-T_\infty\right)}{\rho c_p}\,. \quad (2)$$

If the magnetic domain is established relevant to the transmitting boundary with motion u_0t^n then the momentum Eq. (1) can be written as

$$\frac{\partial u}{\partial t} = \nu\left(1+\frac{1}{\beta}\right)\frac{\partial^2 u}{\partial y^2} + g\beta\left(T-T_\infty\right)\cos(\alpha) - \frac{\sigma B_0^2}{\rho}\left(u-u_0t^n\right). \quad (3)$$

Here $n = 0$ for impulsive motion and $n = 1$ for accelerated motion.

Equations (1) and (3) can be unified into the one equation as

$$\frac{\partial u}{\partial t} = \nu\left(1+\frac{1}{\beta}\right)\frac{\partial^2 u}{\partial y^2} + g\beta\left(T-T_\infty\right)\cos(\alpha) - \frac{\sigma B_0^2}{\rho}\left(u-\lambda u_0 t^n\right). \quad (4)$$

Here $\lambda = 0$ if the magnetic domain is established relevant to the liquid and $\lambda = 1$ if the magnetic domain is established relevant to the moving plate.

The initial and boundary restrictions in dimensional pattern can be written as

$$\left.\begin{aligned} &t=0:\ u=0, && T=T_\infty && \text{for } y\geq 0\\ &t>0:\ u=u_0t^n, && \frac{\partial T}{\partial y}=-\frac{q_w}{k_T} && \text{at } y=0\\ &\quad u\to 0, && T\to T_\infty && \text{as } y\to\infty \end{aligned}\right\}. \quad (5)$$

The radiative flux vector $\boldsymbol{q}_r$ for an optically thin liquid takes the pattern (see [22]):

$$\frac{\partial \boldsymbol{q}_r}{\partial y} = -4a^*\sigma^*\left(T_\infty^4 - T^4\right). \quad (6)$$

Assuming small variance among the liquid temperature T and the autonomous stream temperature T_0 within the flow, T^4 will be expressed as a Taylor's series, regarding to T_0 and omitting the terms of order greater than or equal to two in the series, we have

$$T^4 \cong 4T_\infty^3 T - 3T_\infty^4\,. \quad (7)$$

Using Eqs. (6) and (7) in Eq. (2), we acquired

$$\frac{\partial T}{\partial t} = \frac{k_T}{\rho c_p}\frac{\partial^2 T}{\partial y^2} - \frac{16a^*\sigma^*T_\infty^3\left(T-T_\infty\right)}{\rho c_p} + \frac{Q\left(T-T_\infty\right)}{\rho c_p}\,. \quad (8)$$

The successive non-dimensional variables are initiated

$$\left.\begin{aligned} &U=\frac{u}{\left(u_0\nu^n\right)^{\frac{1}{2n+1}}}, \quad \theta=\left[\frac{u_0}{\nu^{n+1}}\right]^{\frac{1}{2n+1}}\frac{k_T\left(T-T_\infty\right)}{q_w},\\ &Y=\left[\frac{u_0}{\nu^{n+1}}\right]^{\frac{1}{2n+1}}y, \quad \tau=\left[\frac{u_0^2}{\nu}\right]^{\frac{1}{2n+1}}t \end{aligned}\right\}. \quad (9)$$

Equations (4) and (8) modified to the subsequent non-dimensional pattern:

$$\frac{\partial U}{\partial \tau} = \left(1+\frac{1}{\beta}\right)\frac{\partial^2 U}{\partial Y^2} + \mathrm{Gr}\,\theta\cos(\alpha) - m\left(U-\lambda\tau^n\right) \quad (10)$$

$$\frac{\partial \theta}{\partial \tau} = \frac{1}{\mathrm{Pr}}\frac{\partial^2\theta}{\partial Y^2} - (N-H)\theta\,, \quad (11)$$

here $\mathrm{Gr} = \dfrac{g\beta q_w}{k_T}\left[\dfrac{\nu^2}{u_0^4}\right]^{\frac{1}{2n+1}}$, $m = \dfrac{\sigma B_0^2}{\rho}\left[\dfrac{\nu}{u_0^2}\right]^{\frac{1}{2n+1}}$, $\mathrm{Pr} = \dfrac{\nu\rho c_p}{k_T}$,

$N = \dfrac{16a^*\sigma^*T_\infty^3}{\rho c_p}\left[\dfrac{\nu}{u_0^2}\right]^{\frac{1}{2n+1}}$, and $H = \dfrac{Q}{\rho c_p}\left[\dfrac{\nu}{u_0^2}\right]^{\frac{1}{2n+1}}$.

The consequent initial and boundary restrictions can be written as

$$\left.\begin{aligned} &\tau=0:\ U=0, \quad \theta=0 && \text{for } Y\geq 0\\ &\tau>0:\ U=\tau^n, \quad \frac{\partial\theta}{\partial Y}=-1 && \text{at } Y=0\\ &\quad U\to 0,\ \theta\to 0 && \text{as } Y\to\infty \end{aligned}\right\}. \quad (12)$$

3 Solution of the problem

Now, we solve the Eqs. (10) and (11) subject to the initial and boundary restrictions in Eq. (12) by applying Laplace transform technique. We define

$$\eta = \frac{Y}{2\sqrt{\tau}}. \tag{13}$$

Then Eqs. (10) and (11) are transformed into the pattern:

$$\frac{\partial U}{\partial \tau} - \frac{\eta}{2\tau}\frac{\partial U}{\partial \eta} - \left(1+\frac{1}{\beta}\right)\frac{1}{4\tau}\frac{\partial^2 U}{\partial \eta^2} + mU = \mathrm{Gr}\theta\cos(\alpha) + m\lambda\tau^n \tag{14}$$

$$\frac{\partial \theta}{\partial \tau} - \frac{\eta}{2\tau}\frac{\partial \theta}{\partial \eta} - \frac{1}{4\,\mathrm{Pr}\,\tau}\frac{\partial^2 \theta}{\partial \eta^2} + (N-H)\theta = 0. \tag{15}$$

The corresponding boundary conditions can be written as

$$\left.\begin{aligned} &\tau = 0:\ U = 0, \quad \theta = 0 && \text{for } \eta \geq 0 \\ &\tau > 0:\ U = \tau^n, \ \frac{\partial \theta}{\partial \eta} = -2\sqrt{\tau} && \text{at } \eta = 0 \\ &\qquad U \to 0, \quad \theta \to 0 && \text{as } \eta \to \infty \end{aligned}\right\}. \tag{16}$$

The exact solution can be acquired by applying the Laplace transform technique stated as follows:

$$\overline{U}(\eta, p) = \int_0^\infty U(\eta,\tau)\exp(-p\tau)\,d\tau \tag{17}$$

$$\overline{\theta}(\eta, p) = \int_0^\infty \theta(\eta,\tau)\exp(-p\tau)\,d\tau\,. \tag{18}$$

3.1 Impulsive motion

In this case, we take $n = 0$. The exact solutions for the liquid temperature $\theta(\eta, \tau)$ and velocity $U(\eta, \tau)$ are acquired and are displayed in the following pattern after simplification:

$$\theta(\eta,\tau) = a_7\,\psi_2(a_2, \mathrm{Pr}, \eta, \tau) \tag{19}$$

$$\begin{aligned} U(\eta,\tau) &= a_8\,\psi_1(m, a_3, \eta, \tau) + a_9\psi_2(m, a_3, \eta, \tau) \\ &- a_{10}\exp(-a_2\tau)\psi_3(a_2 - m, a_3, \eta, \tau) \\ &- a_{11}\exp(-a_5\tau)\psi_2(m - a_5, a_3, \eta, \tau) \\ &+ \lambda\exp(-m\tau)\psi_1(0, a_3, \eta, \tau) - a_{12}\psi_2(a_2, \mathrm{Pr}, \eta, \tau) \\ &+ a_{13}\exp(-a_5\tau)\psi_2(a_2 - a_5, \mathrm{Pr}, \eta, \tau) + \lambda\left[1 - \exp(-m\tau)\right]. \end{aligned} \tag{20}$$

3.2 Accelerated motion

In this case, we take $n = 1$. The solution procedure runs parallel to the case of impulsive motion. The liquid velocity $U(\eta, \tau)$ in the case of accelerated motion is given by

$$\begin{aligned} U(\eta,\tau) &= \left[a_8\tau + \frac{\lambda}{m}\right]\psi_1(m,\ a_3, \eta, \tau) \\ &+ \left[a_9 + a_{14}\eta\right]\psi_2(m, a_3, \eta, \tau) \\ &- a_{10}\exp(-a_2\tau)\psi_3(a_2 - m, a_3, \eta, \tau) \\ &- a_{11}\exp(-a_5\tau)\psi_2(m - a_5, a_3, \eta, \tau) \\ &- a_{15}\exp(-m\tau)\psi_1(0, a_3, \eta, \tau) - a_{12}\psi_2(a_2, \mathrm{Pr}, \eta, \tau) \\ &+ a_{13}\exp(-a_5\tau)\psi_2(a_2 - a_5, \mathrm{Pr}, \eta, \tau) \\ &- a_{15}\left[1 - \exp(-m\tau)\right] + \lambda\tau. \end{aligned} \tag{21}$$

4 Results and discussion

In this article, the interactive implications of the various parameters such as Casson liquid parameter β, Grashof number Gr, inclination angle α, Hartmann parameter m, time τ, radiation parameter N, and heat generation parameter H on the liquid motion U and temperature θ have been studied analytically and computed results of the analytical solutions are displayed graphically from Figs. 2 to 16. For the purposes of our numerical computations, we adopted the following parameter values: $\beta = 2$, $\mathrm{Gr} = 1$, $\alpha = \pi/4$, $m = 1$, $\tau = 0.5$, $\mathrm{Pr} = 1$, $N = 1$, and $H = 0.5$. To compare our results of liquid motion with those of Chandran et al. [28] as a special case, we computed the numerical values of liquid motion for our problem as well as those of Chandran et al. [28] which are presented in Tables 1 and 2. It is revealed from Tables 1 and 2 that, there is an excellent agreement between both the results.

The impact of Casson parameter on the liquid impulsive motion and accelerated motion is presented in Figs. 2 and 3 at $\lambda = 0$ and $\lambda = 1$ respectively. It is identified that, the liquid motion declines in both cases with an enhancement in the Casson parameter at $\lambda = 0$ and $\lambda = 1$. The nature of Grashof number on the liquid impulsive motion and accelerated motion is presented in Figs. 4 and 5 at $\lambda = 0$ and $\lambda = 1$ respectively. Physically, thermal Grashof number signifies the relative strength of thermal buoyancy force to viscous hydrodynamic force in the boundary layer. It is noticed that, the liquid motion escalates in impulsive and accelerated cases with an increase in the Grashof number at $\lambda = 0$ and $\lambda = 1$. In Figs. 6 and 7 it is observed that, the liquid motion depletes in impulsive and accelerated cases with an enhancement in the angle of inclination at $\lambda = 0$ and $\lambda = 1$.

Figs. 8 and 9 depict the variation of the liquid impulsive motion and accelerated motion with respect to Hartmann number at $\lambda = 0$ and $\lambda = 1$ respectively. It is remarked that, the liquid impulsive motion and accelerated motion escalates in a region near to the plate and depletes in a region away from the plate with an enhancement in the Hartmann number when the magnetic domain is established relevant

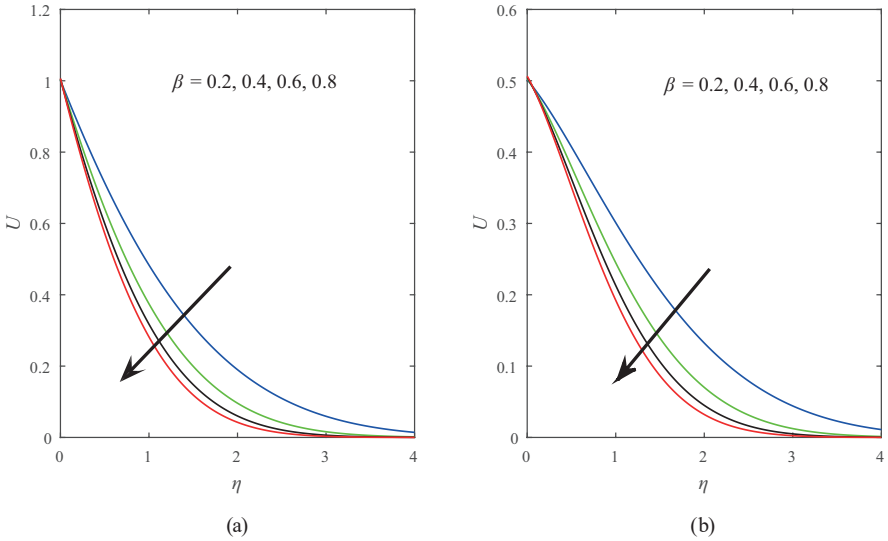

Fig. 2 Consequence of Casson parameter on (a) impulsive motion (b) accelerated motion when $\lambda = 0$

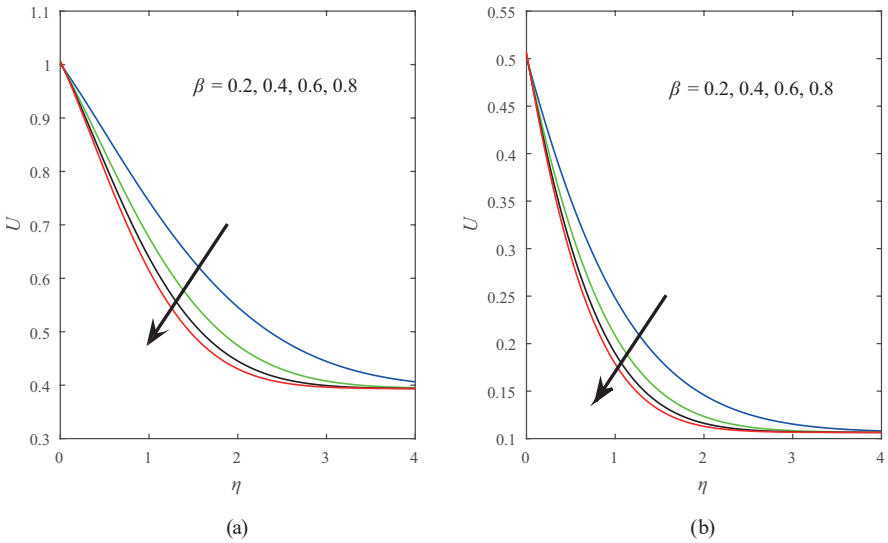

Fig. 3 Consequence of Casson parameter on (a) impulsive motion (b) accelerated motion when $\lambda = 1$

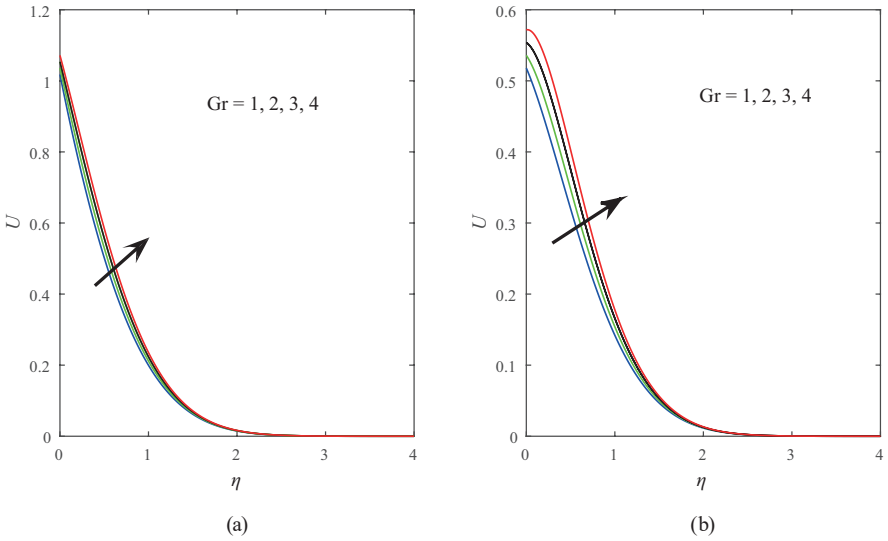

Fig. 4 Consequence of Grashof number on (a) impulsive motion (b) accelerated motion when $\lambda = 0$

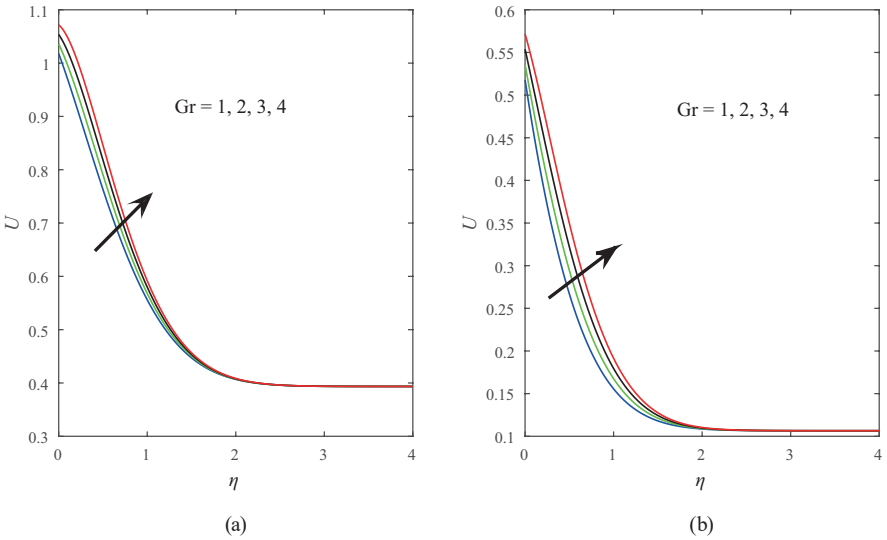

Fig. 5 Consequence of Grashof number on (a) impulsive motion (b) accelerated motion when $\lambda = 1$

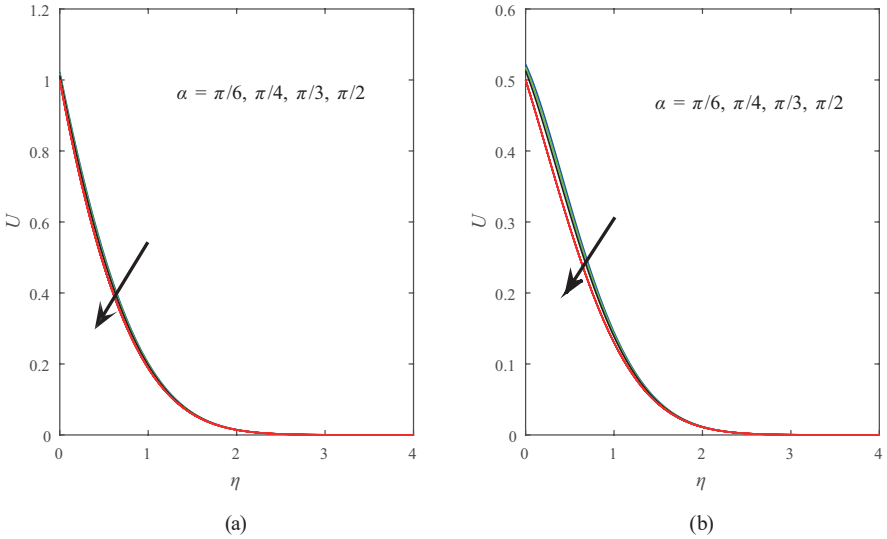

Fig. 6 Consequence of inclined angle on (a) impulsive motion (b) accelerated motion when $\lambda = 0$

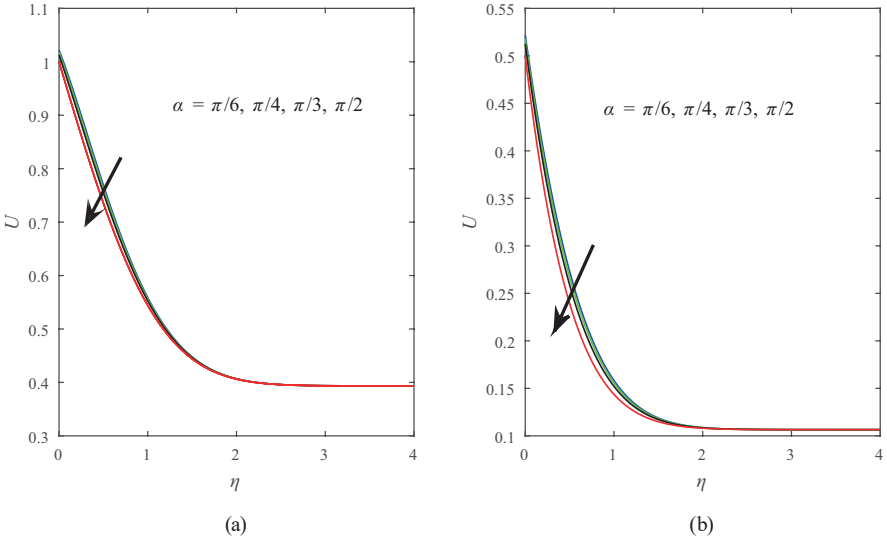

Fig. 7 Consequence of inclined angle on (a) impulsive motion (b) accelerated motion when $\lambda = 1$

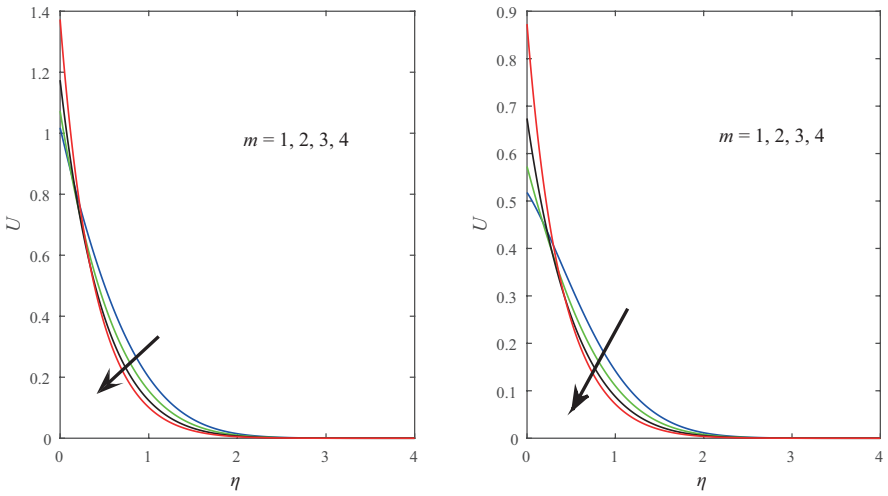

Fig. 8 Consequence of Hartmann parameter on (a) impulsive motion (b) accelerated motion when $\lambda = 0$

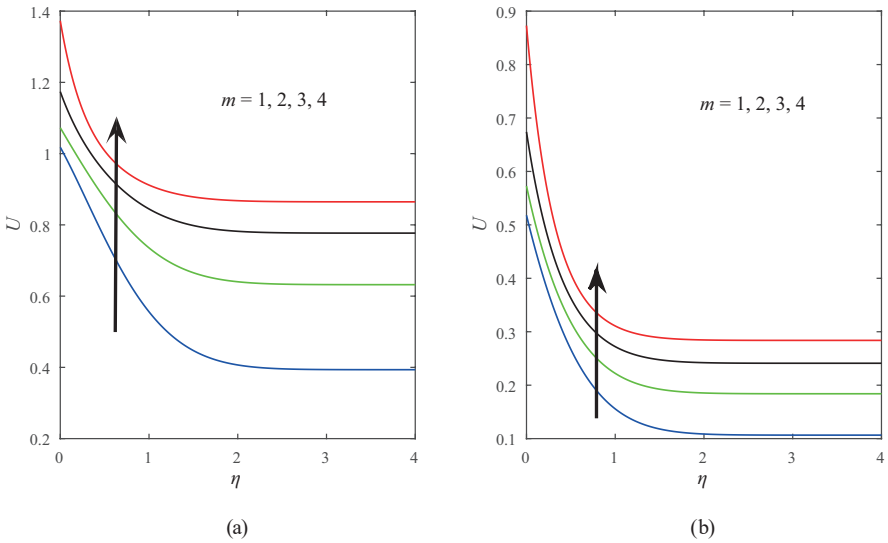

Fig. 9 Consequence of Hartmann parameter on (a) impulsive motion (b) accelerated motion when $\lambda = 1$

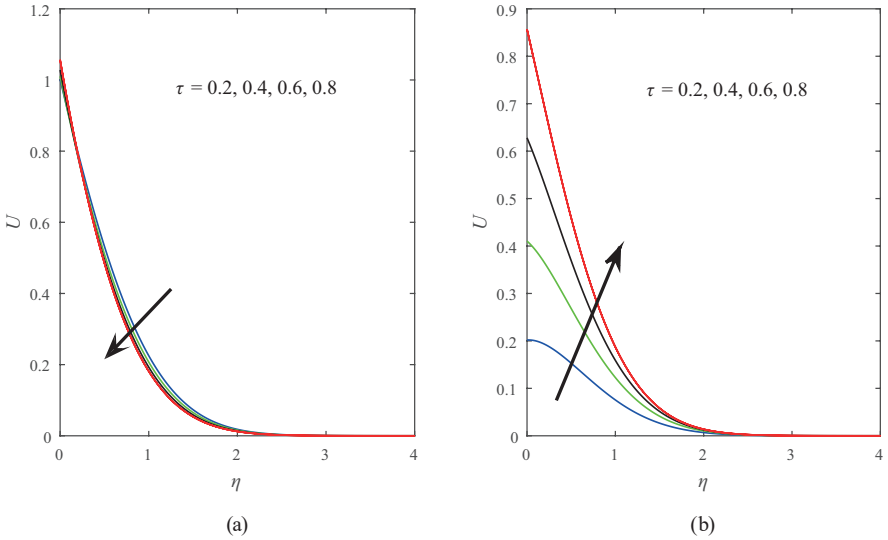

Fig. 10 Consequence of time on (a) impulsive motion (b) accelerated motion when $\lambda = 0$

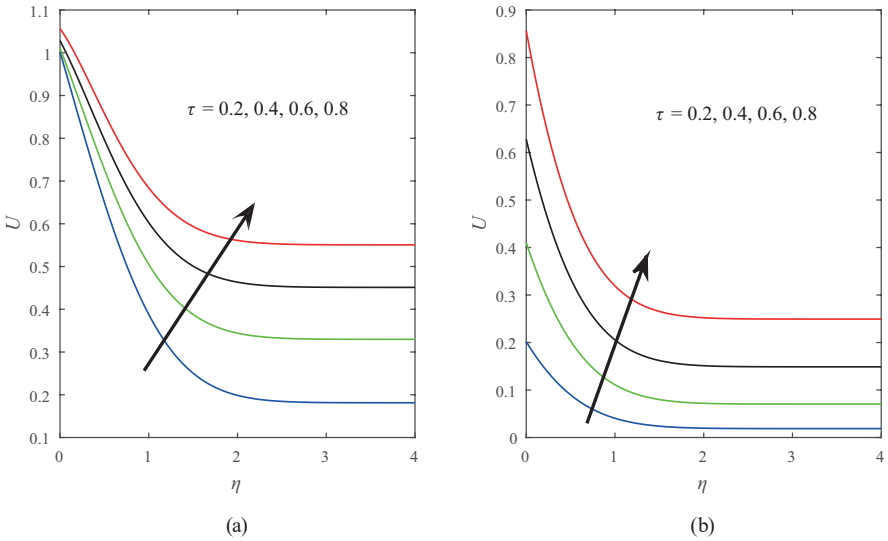

Fig. 11 Consequence of time on (a) impulsive motion (b) accelerated motion when $\lambda = 1$

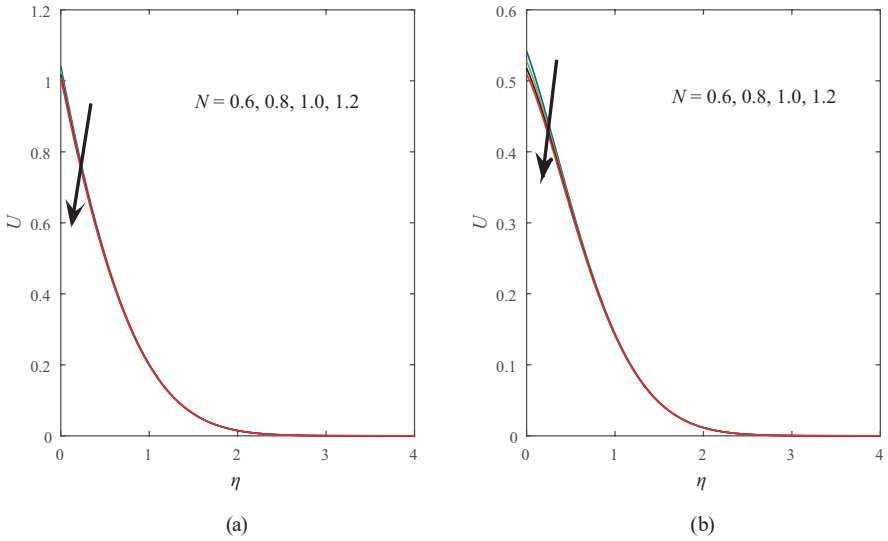

Fig. 12 Consequence of radiation parameter on (a) impulsive motion (b) accelerated motion when $\lambda = 0$

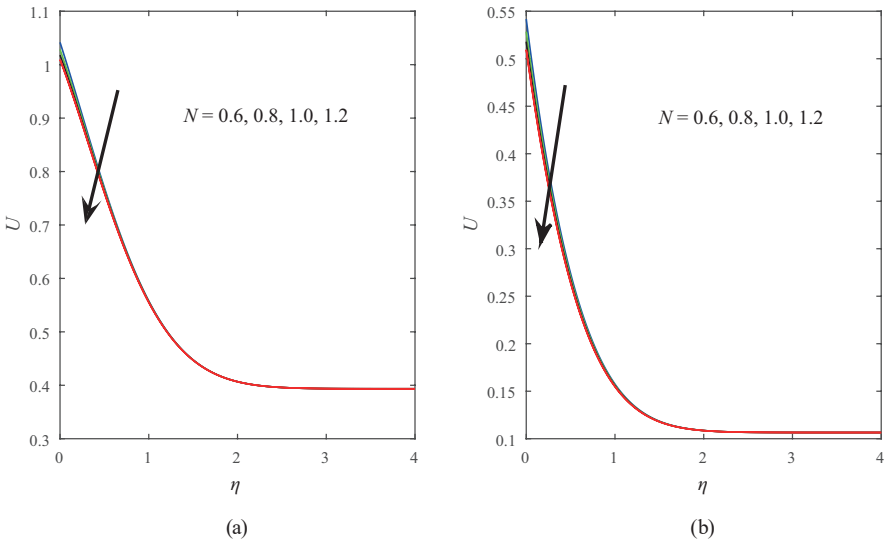

Fig. 13 Consequence of radiation parameter on (a) impulsive motion (b) accelerated motion when $\lambda = 1$

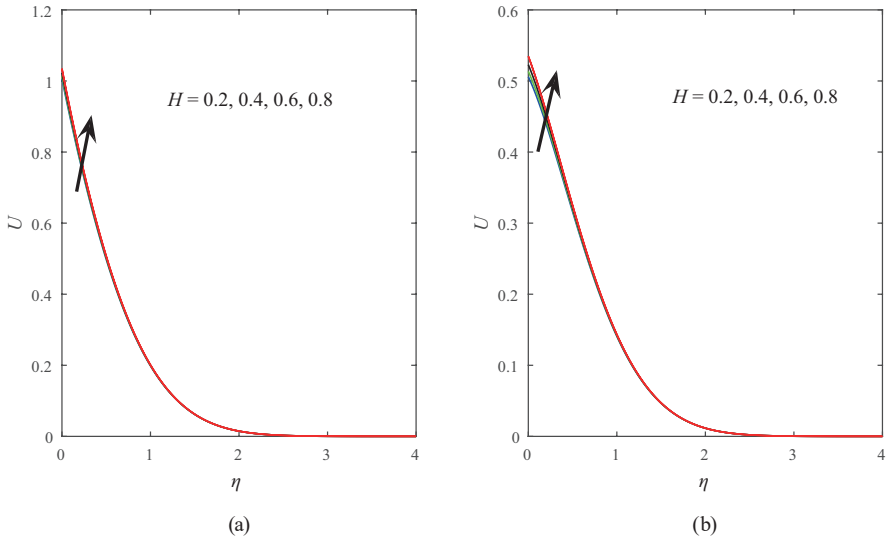

Fig. 14 Consequence of heat generation parameter on (a) impulsive motion (b) accelerated motion when $\lambda = 0$

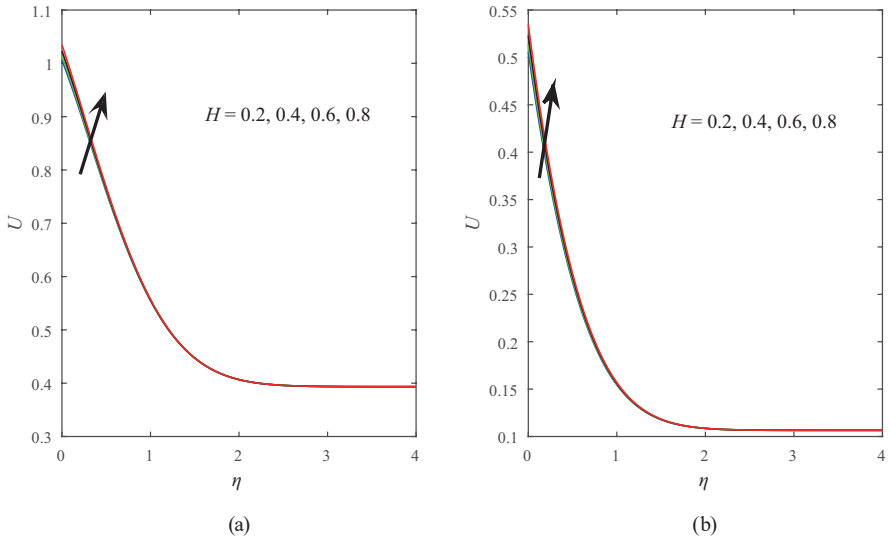

Fig. 15 Consequence of heat generation parameter on (a) impulsive motion (b) accelerated motion when $\lambda = 1$

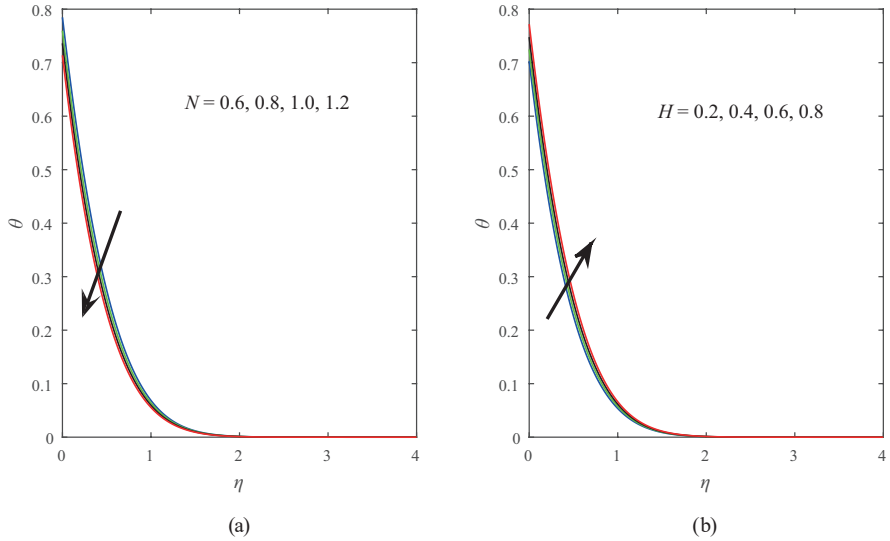

Fig. 16 Consequence of (a) radiation parameter (b) heat generation parameter on the liquid temperature

Table 1 Comparison of the liquid impulsive motion U as $N = 0$, $H = 0$, $\alpha = 0$, Gr = 1, $\tau = 0.1$, and $\beta \to \infty$ with Chandran et al. [28]

	Chandran et al. [28]				Present			
η/m	$\eta = 0$		$\eta = 1$		$\eta = 0$		$\eta = 1$	
	0.1	0.5	0.1	0.5	0.1	0.5	0.1	0.5
0.0	1.000	1.000	1.000	1.000	1.0000	1.0000	1.0000	1.0000
0.2	0.656	0.650	0.662	0.676	0.6561	0.6500	0.6622	0.6761
0.4	0.373	0.366	0.381	0.406	0.3730	0.3660	0.3811	0.4062
0.6	0.181	0.176	0.190	0.222	0.1810	0.1760	0.1901	0.2222
1.8	0.074	0.072	0.084	0.120	0.0740	0.0720	0.0842	0.1201
1.0	0.025	0.025	0.035	0.073	0.0250	0.0250	0.0352	0.0732

Table 2 Comparison of the liquid accelerated motion U as $N = 0$, $H = 0$, $\alpha = 0$, Gr = 1, $\tau = 0.1$, and $\beta \to \infty$ with Chandran et al. [28]

	Chandran et al. [28]				Present			
η/m	$\eta = 0$		$\eta = 1$		$\eta = 0$		$\eta = 1$	
	0.1	0.5	0.1	0.5	0.1	0.5	0.1	0.5
0.0	0.100	0.100	0.100	0.100	0.1000	0.1000	0.1000	0.10000
0.2	0.050	0.050	0.050	0.052	0.0500	0.0500	0.0500	0.0521
0.4	0.023	0.022	0.023	0.025	0.0231	0.0222	0.0231	0.0250
0.6	0.009	0.009	0.009	0.011	0.0091	0.0091	0.0091	0.0110
1.8	0.003	0.003	0.003	0.005	0.0030	0.0030	0.0030	0.0051
1.0	0.001	0.001	0.001	0.003	0.0011	0.0011	0.0011	0.0030

to the liquid ($\lambda = 0$). But the liquid impulsive motion and accelerated motion escalates at all points of the region with an increment in the Hartmann number when the magnetic domain is established relevant to the moving plate ($\lambda = 1$).

Figs. 10 and 11 display the impact of time on the liquid motion in both impulsive and accelerated cases at $\lambda = 0$ and $\lambda = 1$ respectively. It is noticed that, the liquid impulsive motion escalates in a region near to the plate and depletes in a region away from the plate with the progress of time while the accelerated motion escalates at all points of the region with the progress of time when the magnetic domain is established relevant to the liquid ($\lambda = 0$). Both the impulsive motion and accelerated motion of the liquid are raised with the progress of time when the magnetic domain is established relevant to the moving plate ($\lambda = 1$).

It is identified from Figs. 12 and 13 that, the liquid impulsive motion as well as accelerated motion depletes with an enhancement in the radiation parameter at $\lambda = 0$ and $\lambda = 1$. In Figs. 14 and 15 it is remarked that, as the heat generation parameter raises, the liquid impulsive motion and accelerated motion are enhanced at $\lambda = 0$ and $\lambda = 1$. The impact of radiation parameter and heat generation parameter on the liquid temperature is displayed in Fig. 16. It is noticed that, the liquid temperature depletes with an enhancement in the radiation parameter whereas the liquid temperature escalates with an increase of heat generation parameter.

5 Conclusions

The significant observations of this article can be listed as:

- Fluid impulsive motion as well as accelerated motion depletes with an enhancement in the values of Casson liquid parameter, thermal radiation parameter, and angle of inclination for $\lambda = 0$ and $\lambda = 1$.
- Fluid impulsive motion as well as accelerated motion escalates with an enhancement in the values of Grashof number and heat generation parameter for $\lambda = 0$ and $\lambda = 1$.
- There is an increase in a region near to the plate and a deplete in a region away from the plate in the liquid impulsive motion as well as accelerated motion for $\lambda = 0$ whereas there is a reduction in the liquid impulsive motion as well as accelerated motion throughout the channel for $\lambda = 1$ with an enhancement in the value of Hartmann number.
- Fluid temperature declines with the thermal radiation parameter and escalates with the heat generation parameter.

Acknowledgements

It is pleasure to declare our transparent appreciation to the reviewers for their constructive suggestions and comments for renovation of this article.

Nomenclature

a^*	mean absorption coefficient
B_0	uniform magnetic field (Tesla)
c_p	specific heat at constant pressure
Gr	Grashof number
g	acceleration due to gravity (m s^{-2})
H	non-dimensional heat generation parameter
k_T	thermal conductivity of the fluid (m^2 s^{-1})
m	Hartmann parameter
N	radiation parameter
Pr	Prandtl number
Q	dimensional heat generation
$\boldsymbol{q}_r$	radiating flux vector
q_w	heat flux
T	fluid temperature (K)
T_∞	uniform temperature (K)
t	dimensional time (s)
u	fluid velocity in x-direction (m s^{-1})
u_0	characteristic velocity (m s^{-1})
U	scaled velocity (m s^{-1})
v	fluid velocity in y-direction (m s^{-1})

Greek symbols

α	angle of inclination (rad)
β	coefficient of thermal expansion
ρ	fluid density (kg m^{-3})
σ	electrical conductivity (V m^{-1})
τ	non dimensional time (s)
η	scaled coordinate (m)
θ	scaled temperature (K)
σ^*	Stefan-Boltzmann constant

References

[1] Casson, N. "A flow equation for pigment-oil suspensions of the printing ink type", In: Mill, C. C. (ed.) Rheology of Disperse Systems, Pergamon Press, London, UK, 1959, pp. 84–104.

[2] Poornima, T., Sreenivasulu, P., Reddy, N. B. "Slip flow of Casson rheological fluid under variable thermal conductivity with radiation effects", Heat Transfer – Asian Research, 44(8), pp. 718–737, 2015. https://doi.org/10.1002/htj.21145

[3] Aboalbashari, M. H., Freidoonimehr, N., Nazari, F., Rashidi, M. M. "Analytical modeling of entropy generation for Casson nano-fluid flow induced by a stretching surface", Advanced Powder Technology, 26(2), pp. 542–552, 2015. https://doi.org/10.1016/j.apt.2015.01.003

[4] Makinde, O. D., Eegunjobi, A. S. "Entropy analysis of thermally radiating magnetohydrodynamic slip flow of Casson fluid in a microchannel filled with saturated porous media", Journal of Porous Media, 19(9), pp. 799–810, 2016. https://doi.org/10.1615/JPorMedia.v19.i9.40

[5] Reddy, M. G., Kumari, P. V., Padma, P. "Effect of thermal radiation on MHD Casson nanofluid over a cylinder", Journal of Nanofluids, 7(3), pp. 428–438, 2018. https://doi.org/10.1166/jon.2018.1467

[6] Shashikumar, N. S., Prasannakumara, B. C., Archana, M., Geerisha, B. J. "Thermodynamics analysis of a Casson nanofluid flow through a porous microchannel in the presence of hydrody-namic slip: A model of solar radiation", Journal of Nanofluids, 8(1), pp. 63–72, 2019. https://doi.org/10.1166/jon.2019.1568

[7] Gireesha, B. J., Srinivasa, C. T., Shashikumar, N. S., Macha, M., Singh, J. K., Mahanthesh, B. "Entropy generation and heat transport analysis of Casson fluid flow with viscous and Joule heating in an inclined porous microchannel", Proceedings of the Institution of Mechanical Engineers, Part E: Journal of Process Mechanical Engineering, 233(5), pp. 1173–1184, 2019. https://doi.org/10.1177%2F0954408919849987

[8] Kalyan Kumar, C., Srinivas, S. "Influence of Joule heating and thermal radiation on unsteady hydromagnetic flow of chemically reacting Casson fluid over an inclined porous stretching sheet", Special Topics & Reviews in Porous Media: An International Journal, 10(4), pp. 385–400, 2019. https://doi.org/10.1615/SpecialTopicsRevPorousMedia.2019026908

[9] Venkateswarlu, M., Bhaskar. P. "Entropy generation and Bejan number analysis of MHD Casson fluid flow in a micro-channel with Navier slip and convective boundary conditions", International Journal of Thermofluid Science and Technology, 7(4), 070403, 2020. https://doi.org/10.36963/IJTST.2020070403

[10] Goud, B. S., Reddy, Y. D., Rao, V. S., Khan, Z. H. "Thermal radiation and Joule heating effects on a magnetohydrodynamic Casson nanofluid flow in the presence of chemical reaction through a non-linear inclined porous stretching sheet", Journal of Naval Architecture and Marine Engineering, 17(2), pp. 143–164, 2020. https://doi.org/10.3329/jname.v17i2.49978

[11] Cramer, K. R., Pai, S. I. "Magnetofluid dynamics for engineers and applied physicists", McGraw Hill Book Company, 1973. ISBN 9780070134256

[12] Malapati, V., Polarapu, P. "Unsteady MHD free convective heat and mass transfer in a boundary layer flow past a vertical perme-able plate with thermal radiation and chemical reaction", Procedia Engineering, 127, pp. 791–799, 2015. https://doi.org/10.1016/j.proeng.2015.11.414

[13] Yahiaoui, K., Nehari, D., Draoui, B. "The investigation of the mixed convection from a confined rotating circular cylinder", Periodica Polytechnica Mechanical Engineering, 61(3), pp. 161–172, 2017. https://doi.org/10.3311/PPme.9338

[14] Mami, N., Bouaziz, M. N. "Effect of MHD on nanofluid flow, heat and mass transfer over a stretching surface embedded in a porous medium", Periodica Polytechnica Mechanical Engineering, 62(2), pp. 91–100, 2018. https://doi.org/10.3311/PPme.10622

[15] Venkateswarlu, M., Lakshmi, D. V., Makinde, O. D. "Thermodynamic analysis of Hall current and Soret number effect on hydromagnetic Couette flow in a rotating system with a convective boundary condition", Heat Transfer Research, 51(1), pp. 83–102, 2020. https://doi.org/10.1615/HeatTransRes.2019027139

[16] Makinde, O. D., Ogulu, A. "The effect of thermal radiation on the heat and mass transfer flow of a variable viscosity fluid past a vertical porous plate permeated by a transverse magnetic field", Chemical Engineering Communcations, 195(12), pp. 1575–1584, 2008. https://doi.org/10.1080/00986440802115549

[17] Bagheri, S., Roosta, S. T., Heidari, A. "Viscous heating effects on heat transfer characteristics of an explosive fluid in a converging pipe", Periodica Polytechnica Mechanical Engineering, 64(3), pp. 240–247, 2020. https://doi.org/10.3311/PPme.16085

[18] Cao, K., Baker, J. "Non-continuum effects on natural convection–radiation boundary layer flow from a heated vertical plate", International Journal of Heat and Mass Transfer, 90, pp. 26–33, 2015. https://doi.org/10.1016/j.ijheatmasstransfer.2015.05.014

[19] Das, K., Sarkar, A. "Effect of melting on an MHD micropolar fluid flow toward a shrinking sheet with thermal radiation", Journal of Applied Mechanics and Technical Physics, 57(4), pp. 681–689, 2016. https://doi.org/10.1134/S002189441604012X

[20] Ymeli, G. L., Kamdem, H. T. T., Tchinda, R., Lazard, M. "Analytical layered solution of radiation and non-Fourier conduction problems in optically complex media", International Journal of Heat Mass Transfer, 145, 118712, 2019. https://doi.org/10.1016/j.ijheatmasstransfer.2019.118712

[21] Ferroudj, N., Koten, H., Kachi, S., Boudebous, S. "Prandtl number effects on the entropy generation during the transient mixed convection in a square cavity heated from below", Periodica Polytechnica Mechanical Engineering, 65(4), pp. 310–325, 2021. https://doi.org/10.3311/PPme.17563

[22] Venkateswarlu, M., Lakshmi, D. V. "Diffusion-thermo and heat source effects on the unsteady radiative MHD boundary layer slip flow past an infinite vertical porous plate", Journal of Naval Architecture and Marine Engineering, 18(1), pp. 55–72, 2021. https://doi.org/10.3329/jname.v18i1.33024

[23] Alam, M. S., Rahman, M. M., Sattar, M. A. "Effects of variable suction and thermophoresis on steady MHD combined free-forced convective heat and mass transfer flow over a semi-infinite permeable inclined plate in the presence of thermal radiation", International Journal of Thermal Sciences, 47(6), pp. 758–765, 2008. https://doi.org/10.1016/j.ijthermalsci.2007.06.006

[24] Makinde, O. D. "Thermodynamic second law analysis for a gravity-driven variable viscosity liquid film along an inclined heated plate with convective cooling", Journal of Mechanical Science and Technology, 24, pp. 899–908, 2010. https://doi.org/10.1007/s12206-010-0215-9

[25] Venkateswarlu, M., Makinde, O. D. "Unsteady MHD slip flow with radiative heat and mass transfer over an inclined plate embedded in a porous medium", Defect and Diffusion Forum, 384, pp. 31–48, 2018. https://doi.org/10.4028/www.scientific.net/DDF.384.31

[26] Venkateswarlu, M., Bhaskar, P., Venkata Lakshmi, D. "Soret and Dufour effects on radiative hydromagnetic flow of a chemically reacting fluid over an exponentially accelerated inclined porous plate in presence of heat absorption and viscous dissipation", Journal of the Korean Society for Industrial and Applied Mathematics, 23(3), pp. 157–178, 2019. https://doi.org/10.12941/jksiam.2019.23.157

[27] Reddy, K. V., Reddy, M. G., Makinde, O. D. "Heat and mass transfer of a peristaltic electro-osmotic flow of a couple stress fluid through an inclined asymmetric channel with effects of thermal radiation and chemical reaction", Periodica Polytechnica Mechanical Engineering, 65(2), pp. 151–162, 2021. https://doi.org/10.3311/PPme.16760

[28] Chandran, P., Sacheti, N. C., Singh, A. K. "A unified approach to analytical solution of a hydromagnetic free convection flow", [pdf] Scientiae Mathematicae Japonicae, 53(3), pp. 459–468, 2001. Available at: chrome-extension://efaidnbmnnnibpcajpcglclefindmkaj/https://www.jams.jp/scm/contents/Vol-4-6/4-51.pdf [Accessed: 02 September 2021]

Appendix

$$a_1 = 1+\frac{1}{\beta},\ a_2 = N-H,\ a_3 = \frac{1}{a_1},\ a_4 = \frac{\mathrm{Gr}\cos\alpha}{a_1\,\mathrm{Pr}-1},$$

$$a_5 = \frac{a_1a_2-m}{a_1\,\mathrm{Pr}-1},\ a_6 = \frac{a_4}{a_5\sqrt{\mathrm{Pr}}},\ a_7 = \frac{1}{\sqrt{a_2\,\mathrm{Pr}}},\ a_8 = 1-\lambda,$$

$$a_9 = \frac{a_6\sqrt{m}}{a_2},\ a_{10} = \frac{ia_5a_6\sqrt{a_2-m}}{a_2\left(a_2-a_5\right)},\ a_{11} = \frac{a_6\sqrt{m-a_5}}{a_2-a_5},$$

$$a_{12} = \frac{a_6}{\sqrt{a_2}},\ a_{13} = \frac{a_6}{\sqrt{a_2-a_5}},\ a_{14} = \frac{a_8}{2}\sqrt{\frac{a_3}{m}},\ a_{15} = \frac{\lambda}{m},$$

$$\xi_1 = \eta\sqrt{b}-\sqrt{a\tau},\ \xi_2 = \eta\sqrt{b}+\sqrt{a\tau},\ \xi_3 = \eta\sqrt{b}+i\sqrt{a\tau},$$

$$\xi_4 = \eta\sqrt{b}-i\sqrt{a\tau},$$

$$\psi_1(a,b,\eta,\tau) = \frac{1}{2}\begin{bmatrix}\exp\left(-2\eta\sqrt{ab\tau}\right)erfc\left(\xi_1\right)\\+\exp\left(2\eta\sqrt{ab\tau}\right)erfc\left(\xi_2\right)\end{bmatrix},$$

$$\psi_2(a,b,\eta,\tau) = \frac{1}{2}\begin{bmatrix}\exp\left(-2\eta\sqrt{ab\tau}\right)erfc\left(\xi_1\right)\\-\exp\left(2\eta\sqrt{ab\tau}\right)erfc\left(\xi_2\right)\end{bmatrix},$$

$$\psi_3(a,b,\eta,\tau) = \frac{1}{2}\begin{bmatrix}\exp\left(2i\eta\sqrt{ab\tau}\right)erfc\left(\xi_3\right)\\-\exp\left(-2i\eta\sqrt{ab\tau}\right)erfc\left(\xi_4\right)\end{bmatrix}.$$